Contract No:

This document was prepared in conjunction with work accomplished under Contract No. 89303321CEM000080 with the U.S. Department of Energy (DOE) Office of Environmental Management (EM).

Disclaimer:

Hydrogen Permeation Through Radioactive Materials Packaging Components

William R. Johnson* and Kurt Eberl*
* Savannah River National Laboratory

ABSTRACT

Hydrogen permeation through radioactive materials packagings could alleviate conflicting regulatory requirements prohibiting continuous venting but requiring a hydrogen concentration less than the lower flammability limit. This would increase the shipping window duration for many type B packages. Analytical and FE models of hydrogen permeation through a packaging gasket were developed and the flux through the gasket was measured experimentally. From this experiment the diffusivity was measured and used to validate the FE and analytical models of the permeation. These analyses demonstrate a new pathway to show that the hydrogen atmosphere within a package satisfies the regulatory requirements.

INTRODUCTION

Hydrogen permeation through radioactive materials package components could potentially be credited to satisfy the 5% lower flammability limit (LFL) established by the NRC [1] while avoiding the costs of including expensive vents or complex loading processes such as using inerting gases. Hydrogen generation within radioactive materials packages is considered a flammability risk if it exceeds 5% of the container gas void [1]. This generation occurs primarily via radiolysis due to the interaction between alpha radiation and hydrogenous materials such as water or plastic.

According to the Waste Isolation Pilot Plant (WIPP) waste acceptance criteria (WAC) each disposed container is required to have "one or more filter vents or equivalent venting mechanisms [2]" to satisfy the LFL controls imposed by the NRC. For the criticality control overpack (CCO), which is used within the TRU-Pact II for shipping various transuranic wastes and then serving as the waste disposal package at WIPP, an avenue of escape for the hydrogen gas is satisfied using two vents, one on the containment vessel and one on the CCO [3]. At a cost of approximately $100 apiece, if these could be eliminated through crediting hydrogen permeation, a substantial cost savings could be realized.

Hydrogen permeation, to date, is typically not credited as an alternative to venting. Only one similar analysis to that being proposed here, performed on the 9979 Type AF shipping package [4], was found in the literature. For the analysis of the CCO presented here, this study analyzes permeation through a polymer gasket in the internal criticality control container (CCC). Polymers typically have orders of magnitude higher permeability than metals, making this a good candidate as a credited permeation route of hydrogen gas. This paper will first discuss how H_2 diffusion can be modeled analytically, and then how the permeability and Henry's adsorption coefficient were experimentally determined. It will then compare and describe analytical and finite element (FE) models of permeation for the standard ASTM F2378 test for the sealability of gaskets and for the particular gasket used in the CCO.

DIFFUSION MODELING

Analytical Permeation Model

The permeation of gases can be modeled using Fick's laws. Fick's first law states that [5]

$$\vec{F} = -D\nabla\vec{C} \qquad \text{(Eq. 1)}$$

where $\vec{F}$ is the diffusion flux, D is the diffusivity, and $\vec{C}$ is the molar concentration. For the purposes of this analysis, there are only two cases of interest. The first case is when there is a diffusion gradient in only one direction, so that $\nabla \rightarrow \partial/\partial x$, giving

$$F = -D\frac{\partial C}{\partial x} \quad \text{(Eq. 2)}$$

where x is the coordinate through the thickness of the material. The second case is when there is flow out of a cylinder in only the radial direction so that $\nabla \rightarrow \partial/\partial r$ giving that

$$F = -D\frac{\partial C}{\partial r} \quad \text{(Eq. 3)}$$

where r is the radial coordinate. The flow rate through a material can be calculated by multiplying the flux by the cross-sectional area of the material. In the radial case the cross-sectional area used is typically at the outer radius, although at steady state it should be irrelevant what radius is chosen.

Henry's law provides the boundary conditions at the inner and outer surface of the polymer. It states that

$$C_s = K_H P \quad \text{(Eq. 4)}$$

where P is the partial pressure of an adsorptive gas (Pa), K_H is the Henry's adsorption constant (mol/m^{3}Pa), and C_s is the surface concentration (mol/m^3) [6]. For this problem the ideal gas law is applicable.

Experimentally Determining Diffusivity

For the CCO gasket, which is made of an aramid/inorganic with NBR binder, the diffusivity of hydrogen was not well documented, thus tests were needed to experimentally determine it. The tests were conducted using the test setup and procedure described in [7]. To summarize, a sample of a known thickness Δx is placed in between a pressurized volume of gas and a low pressure volume of gas (assume concentration is zero) as shown in Fig. 1. Under these conditions, Eq. 2 reduces to

$$F = -D\frac{C_o - C_i}{\Delta x} \rightarrow F = D\frac{c_i}{\Delta x} \quad \text{(Eq. 5)}$$

where the subscripts o and i indicate the outer and inner surfaces.

The concentration can also be given as a function of the partial pressure, using the ideal gas law. The ideal gas law, stated for the jth species of gas in a mixture, says that

$$P_j V = nRT \quad \text{(Eq. 6)}$$

where P_j is the partial pressure, V is the volume, n is the number of moles of the *j*th species, R is the ideal gas constant, and T is the absolute temperature of the gas. For these experiments, the atmosphere will be assumed to be pure hydrogen, therefore the subscript j for partial pressures can be neglected. Rearranging Eq. 6 gives the concentration

$$C = \frac{n}{V} = \frac{P}{RT} \quad \text{(Eq. 7)}$$

which can then be substituted into Eq. 5 to give the flux as a function of pressure,

$$F = \frac{D}{RT}\frac{P_i}{\Delta x} = DS\frac{P_i}{\Delta x} = \phi\frac{P_i}{\Delta x} \quad \text{(Eq. 8)}$$

where S is the solubility and $\phi = DS$ is the permeability. The permeability is frequently used in practice to combine the diffusivity and solubility.

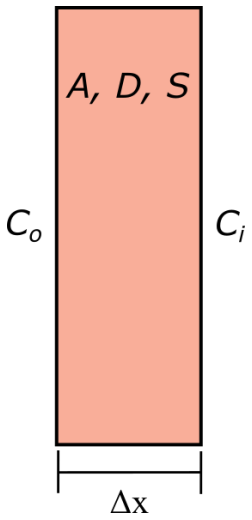

Fig. 1. Test Schematic for Determination of Permeation Properties.

The flow rate Q through the material is given as

$$Q = FA \rightarrow Q = \phi \frac{AP_i}{\Delta x} \quad \text{(Eq. 9)}$$

where A is the cross-sectional area through which the gas is traveling. This can be rewritten to given

$$\frac{Q\Delta x}{A} = \phi P_i. \quad \text{(Eq. 10)}$$

Experimentally, the flow rate Q was measured at several different pressures using deuterium (D_2), as shown in TABLE I. With the cross-sectional thickness and area known, ϕ_{D_2} then becomes the slope of the line given in Eq. 10. A trendline, along with the experimental data is shown in Fig. 2. The permeability for H_2 is $1/\sqrt{2}$ times the permeability of D_2. The measured values are

$$\phi_{D_2} = 3E-6 \ \frac{mol}{m\ Pa\ s}$$

$$\phi_{H_2} = \frac{1}{\sqrt{2}}\phi_{D_2} = 2.12E-6 \ \frac{mol}{m\ Pa\ s}.$$

TABLE I. Permeation Test Experimental Data.

P_i (MPa)	P_i (PSIA)	Q (mol/s)	$Q\Delta x/A$ (mol/s*m)
0.001379	0.2	5.54E-09	4.34E-09
0.002758	0.4	1.09E-08	8.53E-09
0.005516	0.8	2.19E-08	1.72E-08
0.006895	1	2.60E-08	2.04E-08
0.005516	0.8	2.47E-08	1.94E-08
0.004137	0.6	1.83E-08	1.43E-08
0.002758	0.4	1.23E-08	9.66E-09
0.001379	0.2	6.30E-09	4.94E-09

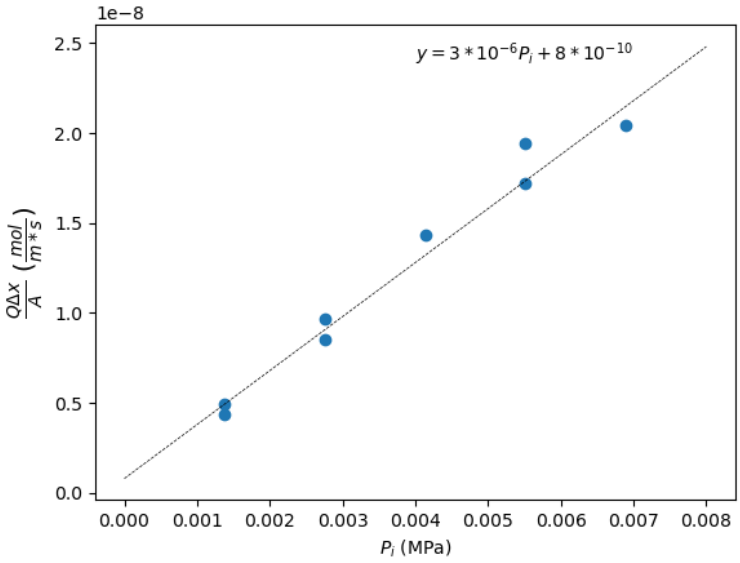

Fig. 2. Permeation Test Experimental Data and Trendline.

Finite Element Model

First an FE model of the test setup to measure the diffusivity was developed. The test, shown in Fig. 1 was performed on a circular material sample with radius 0.0254 m (1 in). The concentration at the outer surface was assumed to be zero, because the vacuum applied to the outer surface evacuates any permeated gas for measurement. Although the internal pressure was known, the Henry's adsorption constant of the material was unknown, therefore the internal boundary condition could not be calculated from the pressure. The internal concentration was deduced by solving Eq. 5 for c_i to give that

$$c_i = \frac{F\Delta x}{D} \qquad \text{(Eq. 11)}$$

which when calculated gave $c_i = 0.0217\ \text{mol/m}^3$. As an added benefit, the Henry's adsorption coefficient could then be calculated as

$$K_H = \frac{c_i}{P} \qquad \text{(Eq. 12)}$$

which for the material examined was found to be 0.0004 mol/m^{3}Pa. When the boundary conditions were applied as described the predicted permeation flow rate was within 0.1% of the measured flow rate.

For the CCC gasket the manufacturer provided a 0.03 cc/min flow rate for nitrogen through a cylindrical disk of gasket material using the ASTM F2378-05 test [8]. A model of this test was created to determine the accuracy of the experimentally measured permeability. The permeation rate of nitrogen (N_2) is approximately 0.16 times the permeation rate of H_2 [9], giving an H_2 permeation rate of 0.1875 cc/min. This test was modeled with finite element analysis (FEA) using the Abaqus mass diffusion step, with the experimentally determined value for ϕ_{H_2}. A schematic of the test is shown in Fig. 3. The ASTM test requires the test gasket to have the geometry shown in TABLE II. Permeation flow rate was available for the maximum press stress in the test, 32 MPa (4640 psi) [10], with an internal pressure of 4 MPa (580 psi).

For the FE model the pressures need to be converted to concentrations to apply as boundary conditions. The concentration at the inner boundary can be calculated using Eq. 4, the 4 MPa prescribed pressure, and the measured Henry's adsorption constant, assuming room temperature (300 K). The outer concentration is assumed to be zero since the permeating atmosphere is constantly being evacuated.

The FEA gasket mesh is shown in Fig. 4 and the predicted mass flux results are shown in Fig. 5, in mol/m^{2}s. To compare the predicted flow rate, the mass flux at the outer surface is multiplied by

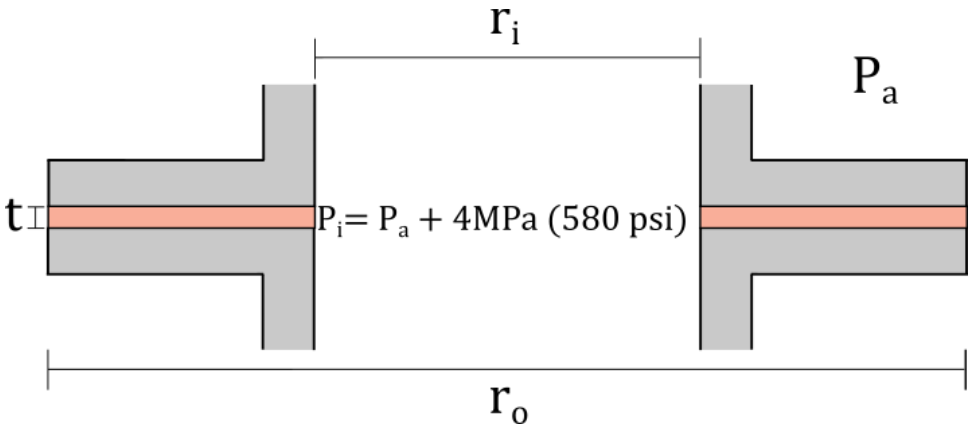

Fig. 3. Schematic of the ASTM F2378 Test for Gasket Sealability.

TABLE II. Dimensions of the ASTM F2378 Test.

Key Dimension	Value
Inner radius r_i	50 mm
Outer radius r_o	90 mm
Thickness t	1.5 mm

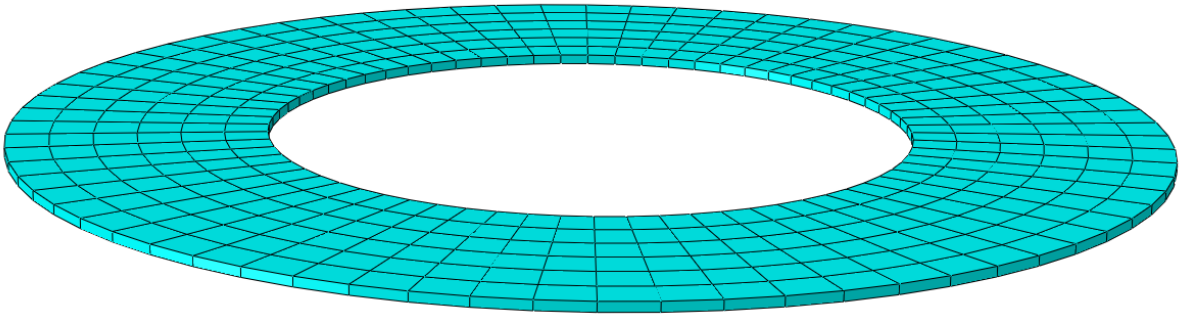

Fig. 4. FEA Mesh for the ASTM F2378 Test.

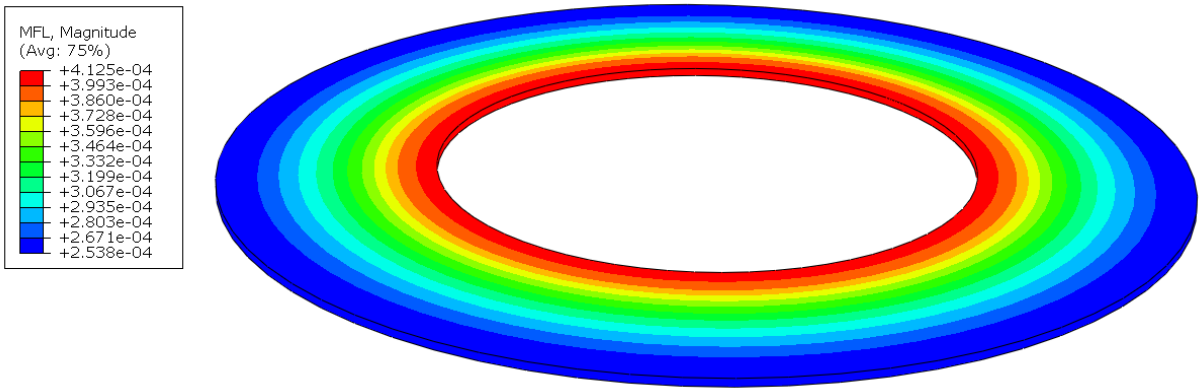

Fig. 5. ASTM F2378 FE Predicted Mass Flux Magnitude (mol/m^{2}s).

the outer surface area and then converted to a volumetric flow rate in cc/min using the ideal gas law. The predicted volumetric flow rate is 0.319 cc/min, which is 1.7 times the expected flow rate of 0.1875 cc/min. This difference may be due to the difference in the press stress used in the ASTM F2378 test and the experiment used to determine the permeability, which had no applied press stress. Although this prediction isn't perfect, because hydrogen permeation rates through materials can vary widely, this prediction is accurate enough to give confidence in the modeling process.

CCC Gasket Model

For the CCC, the hydrogen generation rate was assumed to be 3.72×10^{-6} mol/s, a conservative value provided by [11], and larger than any of the approved content values for the packages of the TRUPACT-II [3]. The gasket dimensions are given in TABLE III. Eq. 9 was used to predict the permeation flow rate through the gasket, with the permeability $\phi_{H_2} = 2.12e-6$ mol/m Pa s. The cross sectional area was calculated at the outside edge of gasket as $A = 2\pi r_o t$. Because the form of Fick's law is the same for both the $\partial/\partial x$ and $\partial/\partial r$, in Eq. 9 $\Delta x = \Delta r = r_o - r_i$.

TABLE III. Dimensions of the CCC Gasket.

Key Dimension	Value
Inner radius r_i	84.1375 mm (3.3125 in)
Outer radius r_o	107.95 mm (4.25 in)
Thickness t	4.6355 mm (0.1825 in)

The flow rate out of the CCC gasket, as a function of volume fraction up to 5% is shown in Fig. 6. The dashed line shows the hydrogen generation rate, while the blue line shows the permeation rate. Because permeation through a material is driven by pressure difference, at volume ratios close to 0 almost no permeation occurs. However, as the volume ratio increases, the permeation flow rate also increases. At 0.25% the permeation rate is approximately the same as the hydrogen generation rate. By the 5% volume ratio LFL the permeation rate is approximately 19.5 times larger than the hydrogen generation rate. Because the generation rate and permeation flow rate are the same around 0.25% the amount of hydrogen within the package would never exceed this value, and 5% LFL would never be reached. If the flow rate were lower by a factor of 1.7, the flow rate would still be approximately 11.5 times the generation rate.

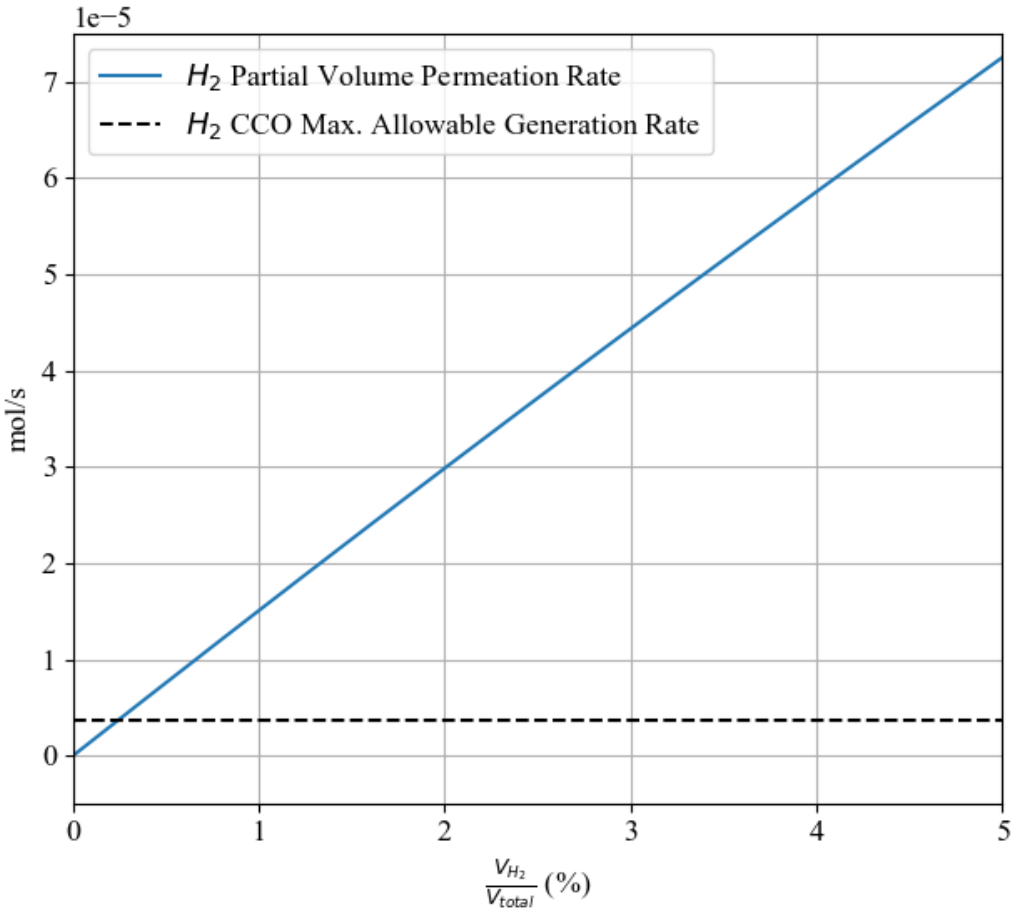

Fig. 6. Hydrogen Permeation as a Function of Volume Ratio.

CONCLUSION

Hydrogen permeation through a polymer gasket was investigated to determine whether or not the permeation could satisfy the 5% LFL imposed by the NRC while also acting as an equivalent venting mechanism for the WIPP WAC. Analytical and FE models of hydrogen permeation were presented to predict the permeation rate. The permeability of the gasket material was measured experimentally and the flow rate was predicted. The predicted flow rate showed that the permeability through the gasket was more than sufficient to allow for the flow of hydrogen out of the CCC given a conservative hydrogen generation rate.

Although this work shows that the gasket permeation would be sufficient to allow for the escape of hydrogen, it is not on a conservatively bounding case. The permeability, along with being press stress dependent, is also temperature dependent. This study was carried out at STP, while radioactive materials packages must be able to maintain containment down to -40°C, the most unfavorable operational condition for permeation that radioactive materials packages must be certified for [12]. Our experimental apparatus is currently being upgraded to measure the permeability of materials at low temperatures, which will make the prediction of permeation under this condition possible as well.

REFERENCES

1. Nuclear Regulatory Commission “Clarification of conditions for waste shipments subject to hydrogen gas generation” Information Notice 84-72 (1984)
2. *Transuranic Waste Acceptance Criteria for the Waste Isolation Plant*, DOE/WIPP-02-3122, Rev.

10, August 2020.
3. *CH-TRU Payload Appendices*, Rev. 4, August 2020
4. Joshua P. Flach, Paul S. Blanton, and Don S. Hoang "Evaluation of hydrogen gas generation and permeation in the 9979 Type AF shipping package" *Proceedings of the 2020 Pressure Vessels and Piping Conference* (2020)
5. J. Crank *The Mathematics of Diffusion, 2nd ed.* Clarendon Press (1975)
6. Endre Nagy *Basic Equations of Mass Transport Through a Membrane Layer (2nd ed.), Ch. 18 Membrane Gas Separation*, Elsevier 2018
7. Katherine T. Young, Timothy M. Krentz, Anna L. d'Entremont, Eric M. Vogel, and Dale A. Hitchcock "Measurement of gas-concentration-driven permeation for the examination of permeability, solubility, and diffusivity in varying materials" *Review of Scientific Instruments* 91 (2020)
8. "ASTM F2378-05: Standard test method for sealability of sheet, composite, and solid form-in-place gasket materials" *ASTM International* 2016
9. Junius D. Edwards and S. F. Pickering "Permeability of rubber to gases" *Scientific Papers of the Bureau of Standards* 16 (1920)
10. *Durlon 8500,* Gasket Resources Inc., Downington PA, 10/16/2020
11. M. Devarakonda, C. Morrison, and M. A. Italiano "Efforts to update the TRUPACT-II hydrogen and gas generation model" Waste Management Symposia, March 2004.
12. United States Nuclear Regulatory Commission "Packaging and Transportation of radioactive Material - Hypothetical accident conditions, 10 CFR 71.43, as amended